Journal of Power Sources 187 (2009) 57–66

Contents lists available at ScienceDirect

Journal of Power Sources

journal homepage: www.elsevier.com/locate/jpowsour

Hybrid inorganic–organic proton conducting membranes based on Nafion and 5 wt% of M_xO_y (M = Ti, Zr, Hf, Ta and W). Part II: Relaxation phenomena and conductivity mechanism

Vito Di Noto[a,b,*], Sandra Lavina[a], Enrico Negro[a], Michele Vittadello[c], Fosca Conti[a], Matteo Piga[a], Giuseppe Pace[d]

[a] Dipartimento di Scienze Chimiche,Università di Padova, Via Marzolo 1, 35131 Padova (PD), Italy
[b] Istituto di Scienze e Tecnologie Molecolari, ISTM-CNR c/o Dipartimento di Scienze Chimiche, Via Marzolo 1, 35131 Padova (PD), Italy
[c] Department of Materials Science & Engineering, Rutgers University, 607 Taylor Road, Piscataway, NJ, USA
[d] Istituto di Scienze e Tecnologie Molecolari, ISTM-CNR c/o Dipartimento di Processi Chimici dell'Ingegneria, Via Marzolo 9, 35131 Padova (PD), Italy

ARTICLE INFO

Article history:
Received 9 May 2008
Received in revised form 8 July 2008
Accepted 19 October 2008
Available online 28 October 2008

Keywords:
Hybrid inorganic–organic proton conducting membranes
Nafion
Fuel cells
Differential scanning calorimetry
Dynamical mechanic analysis
Broadband dielectric spectroscopy

ABSTRACT

In this report, we are presenting studies of the effect of M_xO_y nanopowders on the thermal, mechanical and electrical properties of [Nafion/$(M_xO_y)_n$] membranes with M = Ti, Zr, Hf, Ta and W and n = 5 wt%. Five homogeneous membranes with thicknesses ranging from 170 to 350 μm were studied. The thermal transitions characterizing [Nafion/$(M_xO_y)_n$] materials were investigated by modulated differential scanning calorimetry (MDSC). The mechanical parameters and relaxation processes were studied on temperature by dynamical mechanical analyses (DMA). Broadband dielectric spectroscopy (BDS) was used to study the conductivity mechanism and dielectric relaxation events in bulk materials. DMA investigations showed two distinct relaxation events. The first relaxation phenomenon, detected at about 19 °C, was attributed to the mechanical β-relaxation mode of Nafion. The second event, revealed in the temperature range 100–135 °C, was assigned to the mechanical α-relaxation mode of Nafion. The electric response of membranes was studied by BDS measurements in the frequency and temperature range respectively of 40 Hz–10 MHz and 5–135 °C. Real and imaginary components of permittivity ($\varepsilon^*(\omega) = \varepsilon'(\omega) - i\varepsilon''(\omega)$) and conductivity spectra ($\sigma^*(\omega) = \sigma'(\omega) + i\sigma''(\omega)$) were analyzed. Conductivity spectra allowed us to accurately determine the σ_{dc} of membranes at 100% RH as a function of T. Two relaxation peaks were detected in the $\varepsilon^*(\omega)$ profiles. The low frequency relaxation event was attributed to the α-relaxation mode of fluorocarbon chains of Nafion. The high frequency relaxation peak corresponds to the β-relaxation of acid side groups. The results allowed us to conclude that M_xO_y influences: (a) the relaxations of both the hydrophobic and the hydrophilic domains of Nafion polymer host; (b) the thermal stability range of conductivity (SRC) and the σ_{dc} of membranes.

In conclusion, nanofillers affect the macromolecular dynamics of Nafion-based polymer host owing to the formation of dynamic cross-links, R–$SO_3H\cdots M_xO_y\cdots HSO_3$–R, in hydrophilic polar cages. The membranes doped with HfO_2 and WO_3 oxoclusters present a stability range of conductivity of $5\,^{\circ}C \leq T \leq 135\,^{\circ}C$ and give rise to σ_{dc} values of respectively 2.8×10^{-2} and 2.5×10^{-2} S cm^{-1} at 135 °C and 100% RH. These latter conductivity values make the nanocomposite membranes based on HfO_2 and WO_3 oxoclusters very promising materials for the application in polymer electrolyte fuel cells (PEMFCs) and direct methanol fuel cells (DMFCs).

1. Introduction

During the last decades, the increment of oil prices has brought back into focus the need to carry out research on fuel cells [1–5]. The growing awareness on environmental issues is an additional factor pressing researchers to improve these systems up to commercial standards [1–5]. Direct methanol fuel cells (DMFCs) are generally considered the most appropriate to lead the transition

* Corresponding author at: Dipartimento di Scienze Chimiche,Università di Padova, Via Marzolo 1, 35131 Padova (PD), Italy. Tel.: +39 0498275229; fax: +39 0498275229.
E-mail address: vito.dinoto@unipd.it (V. Di Noto).

0378-7753/$ – see front matter © 2008 Elsevier B.V. All rights reserved.
doi:10.1016/j.jpowsour.2008.10.066

toward the hydrogen economy [1]. Unfortunately, there are still some major drawbacks that need to be addressed in these systems, including: (a) costs; (b) low proton conductivities above 100 °C and low humidity; (c) methanol crossover.

Nafion still represents the standard among proton conducting membranes [6–8]. This material successfully arises from a combination of sulfonic acidity with a perfluorinated polymer network with which it is hard to compete. However, Nafion is not exempt from the decrement of conductivity due to loss of hydration, methanol crossover and high cost issues [7–8]. The well-known reliability of this system at low temperatures has prompted several studies aimed at improving its properties anyway [9–15]. Significant efforts have been directed toward the synthesis of organic–inorganic composites based on Nafion and micrometric/nanometric inorganic fillers [9–13]. The introduction of particles such as SiO_2, zirconium phosphate, phosphotungstic acid, molybdophosphoric acid, aerosil-SiO_2, organically modified silicates, silane-based fillers, zeolites seems to overcome the drawbacks of Nafion [9–13]. Previous research in our group [16] has elucidated the effects of silica concentration in [Nafion/$(SiO_2)_x$] nanocomposite membranes with $0\,wt\% \le x \le 15\,wt\%$. It has been shown how the inorganic fillers and different water species affect the dynamic relaxations of Nafion and consequently the conductivity mechanism. It was demonstrated [16] that SiO_2 oxoclusters modulate the relaxations of both the hydrophobic (R_{fd}) and hydrophilic (R_c) components of Nafion polymer host. The formation of dynamic cross-links $SiO_2\cdots HSO_3-$ in hydrophilic polar clusters influence the macromolecular dynamics of hydrophobic fluorocarbon domains of the host material. These investigations were extended to the structural, morphological and thermal characterization of [Nafion/$(M_xO_y)_n$] membranes with M = Ti, Zr, Hf, Ta and W and $n = 5$ wt% [17]. In particular, vibrational spectroscopy measurements have shown that these membranes consist mostly of fluorocarbon chains with helical conformation 15_7, with a smaller amount of 10_3 helixes dependent on the metal oxide types [17]. Four different species of water domains were detected in [Nafion/$(M_xO_y)_n$] materials, namely: (a) bulk water [$(H_2O)_n$]; (b) water solvating oxonium ions directly interacting with the sulphonic anion side group, [$H_3O^+\cdots{}^-SO_3-$]·$(H_2O)_n$; (c) acid water, [$H_3O^+\cdots(H_2O)_n$]; and (d) water molecules interacting with metal oxoclusters, [$M_xO_y\cdots(H_2O)_n$]. It was revealed [17] that the amount of each type of water domain in the bulk membranes depends on the acidity of M_xO_y oxoclusters. Furthermore, it was shown [17] that these materials are characterized by a thermal stability up to 170 °C.

In this paper are presented accurate BDS, DMA and MDSC investigations performed on [Nafion/$(M_xO_y)_n$] membranes with M = Ti, Zr, Hf, Ta and W and $n = 5$ wt%.

It should be noted that, before starting this study many attempts were performed by preparing hybrid [Nafion/$(M_xO_y)_n$] materials with a fixed molar ratio M_xO_y/–SO_3H or with a constant filler volume fraction. Nevertheless, in order to carefully investigate the effect of different metal ion oxoclusters on the physicochemical properties of hybrid materials the best compromise was obtained by preparing membranes characterized with a constant filler weight percentage for the following reasons. First, very homogeneous [Nafion/$(M_xO_y)_n$] membranes are obtained when the concentration of filler is in the order of 5 wt%. Furthermore, on the basis of the density values of M_xO_y oxoclusters [17], in this latter condition, the molar ratio $\psi = (mol_{M_xO_y})/(mol_{-SO_3H})$ is varying in [Nafion/$(M_xO_y)_n$] within the same order of magnitude ($0.14 \le \psi \le 0.78$). Second, the different morphology and average particle size of M_xO_y fillers [17] makes very difficult the preparation of hybrid membranes with a constant and reproducible volume fraction. The preparation and the structural analyses of materials are described in the first part of this study [17]. The present report is focused on the microscopic investigation of ion transport dynamics and dielectric relaxation events in bulk [Nafion/$(M_xO_y)_n$] materials. Particularly, the aim of these studies was to reveal the influence of the oxocluster–polymer interactions on: (a) the R_c relaxation phenomena [16] happening in the hydrophilic domains of Nafion host material; and (b) the R_{fd} relaxation events [16] occurring in hydrophobic fluorocarbon domains of host polymer. The results are correlated with structural information and properties of membranes described in the first part of this study [17].

2. Experimental

[Nafion/$(M_xO_y)_n$] nanocomposite membranes with $n = 5$ wt% and M = Ti, Zr, Hf, Ta and W were prepared by a solvent casting procedure as described earlier [17]. The thicknesses of the prepared membranes were in the range 170–350 μm. Activation, purification and thermal reference condition of analyzed membranes were obtained as described previously [17]. The proton exchange capacity (PEC), the φ parameter and the molar ratios ψ_M of materials were reported elsewhere [17]. PEC is the proton exchange capacity of the polymer matrix, while φ is the overall proton exchange capacity of the hybrid membrane. In particular, φ is given by

$$\varphi = \frac{\left(meq_{Nafion} + \sum_{M_xO_y} meq_{M_xO_y}\right)}{w_{composite}} = PEC f_{Nafion} + \sum_{M_xO_y} PEC_{M_xO_y} f_{M_xO_y},$$

where $f_i = w_i/w_{composite}$, with i = Nafion or M_xO_y, is the weight fraction of each component. w_i and $w_{composite}$ are the weight respectively of the i-th component and of the hybrid material. $PEC_{M_xO_y}$ is the proton exchange capacity of M_xO_y filler. ψ_M singles out the molar ratio M_xO_y/–SO_3H of nanocomposite materials.

Modulated differential scanning calorimetry (MDSC) measurements were carried out with a MDSC 2920 differential scanning calorimeter (TA Instruments) equipped with the LNCA low-temperature attachment operating under a helium flux of 30 $cm^3\,min^{-1}$. Measurements were performed with a heating rate of 3 °C min^{-1} in the range $-50\,°C < T < 350\,°C$ on about 4 mg of a sample sealed in an aluminium pan. Before the measurements were taken, materials were dried for 1 h under air at $T = 30$ °C.

Dynamic mechanical analyses (DMA) were carried out with a TA Instruments DMA Q800 using the film/fiber tension clamp. Temperature spectra in the −10 to 210 °C range at a rate of 4 °C min^{-1} were determined subjecting a rectangular film sample of ca. 25(height) × 6(width) × 0.2(thickness) mm^3 to an oscillatory sinusoidal tensile deformation at 1 Hz with an amplitude of 4 μm and a preload force of 0.05 N. Before measurements the samples were dried for 24 h in air at 80 °C. The mechanical response data were analyzed in terms of the elastic (storage) modulus (E') and viscous (loss) modulus (E''). $\tan\delta = E''/E'$ was analyzed on temperature in order to reveal the mechanical relaxation phenomena.

Electrical spectra were measured in the 40 Hz–10 MHz frequency range using an Agilent 4294A Impedance Analyzer. The temperature range from 5 to 135 °C was explored by using a Novocontrol Quatro cryostat operating with an N_2 gas jet heating and cooling system. As described in detail elsewhere [18], the measurements were performed by sandwiching the fully hydrated samples between two circular platinum electrodes sealed within a CR2032 button battery case with a free volume of ca. 0.3 cm^3. The geometrical constant of the cell was obtained by measuring the electrode–electrolyte contact surface and the distance between electrodes with a micrometer. No corrections for thermal expansion

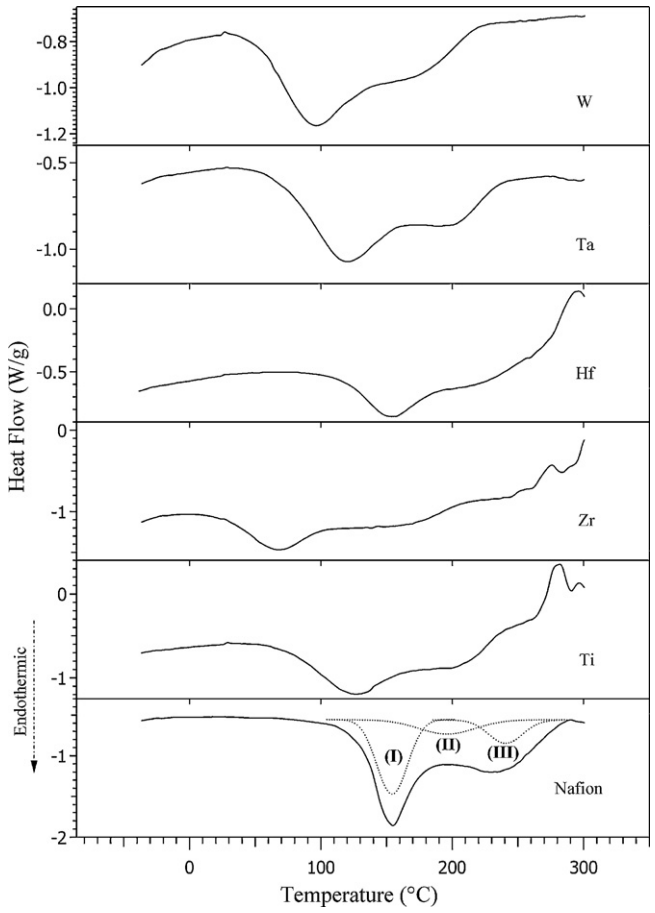

Fig. 1. MDSC curves of [Nafion/$(M_xO_y)_n$] with $n = 5$ wt% and M = Ti, Zr, Hf, Ta and W. Decomposition by Gaussian functions of MDSC region in the 90–300 °C range is shown. I, II and III indicate the detected endothermic peaks.

of the cell were carried out. The temperature was measured with accuracy greater than ±0.1 °C. The complex impedance ($Z^*(\omega)$) was converted into complex conductivity ($\sigma^* = \sigma' + i\sigma''$) and permittivity ($\varepsilon^* = \varepsilon' - i\varepsilon''$) as described elsewhere [16,18].

σ^* spectra were employed to measure accurately the conductivity of samples, σ_{dc}, as described previously [16,18].

3. Results and discussion

3.1. Differential scanning calorimetry

The first MDSC scan of [Nafion/$(M_xO_y)_n$] systems, shown in Fig. 1, yielded three intense overlapping endothermic peaks in the 50–280 °C temperature range. These transitions, in accordance with other studies [16], were indicated as I, II and III (Fig. 1 and Table 1). The peak position depends on the oxocluster used in the preparation of [Nafion/$(M_xO_y)_n$] materials. In particular, for pristine Nafion, the onset temperatures for events I, II and III are detected at ca. 122, 168 and 181 °C, respectively. I was assigned to the order–disorder molecular rearrangement transitions which occur due to thermal relaxation processes taking place inside Nafion's hydrophilic polar clusters. This peak is diagnostic for the anion–cation and acid side groups–water interactions inside Nafion polar cages. The highest onset temperatures of peak I was observed for both pristine Nafion and [Nafion/$(HfO_2)_n$] membranes (Fig. 1 and Table 1). These results suggest that $M_xO_y\cdots^-SO_3$–R interactions occurring in [Nafion/$(M_xO_y)_n$] with M ≠ Hf reduce the thermal stability of hydrophilic polar clusters.

Table 1
MDSC transition temperatures of [Nafion/$(M_xO_y)_n$] membranes with $n = 5$ wt%.

M_xO_y	Peak (I) (°C)		Peak (II) (°C)		Peak (III) (°C)	
	Onset	Minimum	Onset	Minimum	Onset	Minimum
–	122	155	168	194	181	234
TiO_2	75	121	174	203	246	263
ZrO_2	30	67	105	160	215	254
HfO_2	112	153	182	213	220	260
Ta_2O_5	78	119	177	206	261	255
WO_3	48	98	140	180	221	275

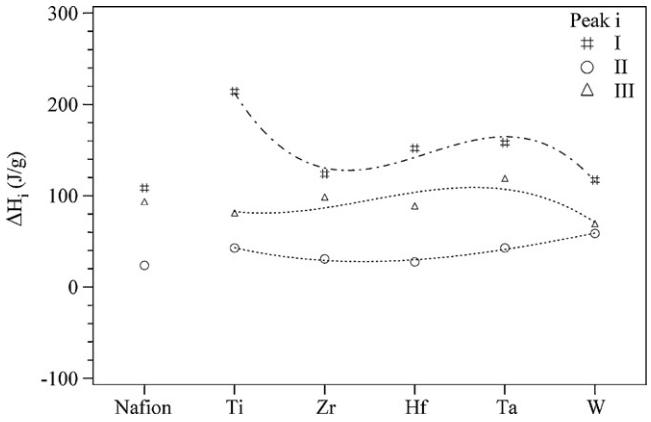

Fig. 2. Dependence on M of ΔH_i (J/g) of I, II and III endothermic peaks.

In accordance with other studies [16]: (a) peak II, revealed in the 150–250 °C temperature range (Fig. 1, Table 1), was assigned to the endothermic decomposition of sulfonic acid groups; and (b) peak III, detected in the 200–300 °C temperature range (see Fig. 1, Table 1), was attributed to the melting transition of hydrophobic fluorocarbon microcrystalline regions of Nafion.

MDSC results, which are in accordance with thermogravimetric studies reported elsewhere [17], revealed that in the [Nafion/$(M_xO_y)_n$] membranes with M ≠ Hf, the R–$SO_3H\cdots M_xO_y$ interactions act to reduce the thermal stability of both polar hydrophilic clusters and hydrophobic PTFE backbone domains. These results were supported by ΔH values of events I, II and III (Fig. 2). ΔH of peaks was evaluated by decomposition of MDSC curves with Gaussian functions. Fig. 2 shows that: (a) ΔH_I and ΔH_{II} of composite membranes are slightly higher than those of pristine Nafion, thus confirming that $M_xO_y\cdots HSO_3$– interactions occur in the hydrophilic ionic cages of membranes; (b) ΔH_{III} is quite constant and similar to that of Nafion. As expected, this latter evidence demonstrates that the melting of fluorocarbon domains is independent of the M_xO_y used in the preparation of [Nafion/$(M_xO_y)_n$] membranes.

Taken together, MDSC results indicated that: (a) the M_xO_y oxoclusters are involved in the dynamic cross-links R–$SO_3H\cdots M_xO_y\cdots HSO_3$–R, which take place in hydrophilic ionic cages of composite membranes; and (b) the most thermally stable membrane is that based on HfO_2.

3.2. Dynamic mechanical analysis

The effect of M_xO_y on mechanical properties of membranes was studied by carefully analyzing the temperature spectra of the storage modulus (E'), loss modulus (E'') and tan δ. Measurements were carried out using a dynamic oscillatory method where small sinusoidal mechanical elongations of 4 μm at 1 Hz of frequency were applied to the sample. Fig. 3 shows the logarithms of the storage

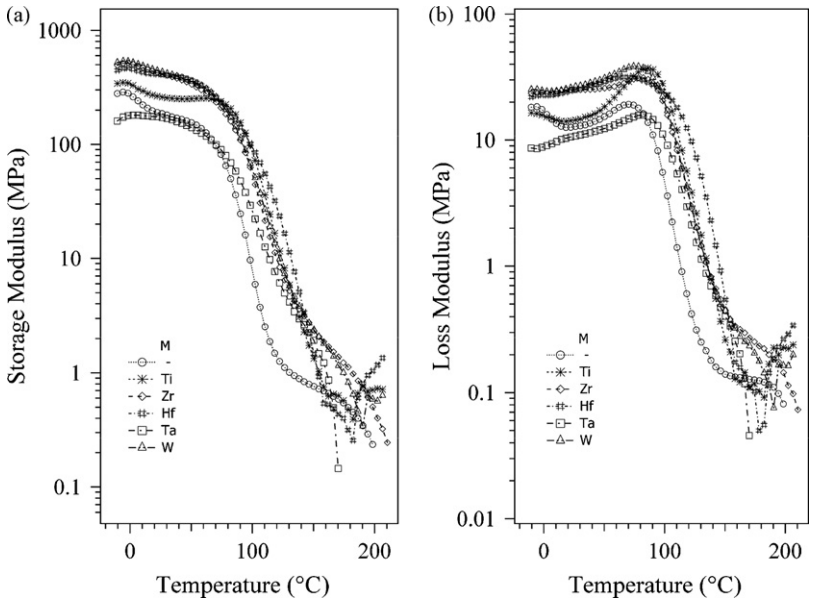

Fig. 3. Temperature spectra of storage modulus (E', panel a) and loss modulus (E'', panel b) for [Nafion/(M_xO_y)$_n$] with n = 5 wt% and M = Ti, Zr, Hf, Ta and W.

and loss modulus on temperature of [Nafion/(M_xO_y)$_n$] materials. At 100 °C the α-relaxation of Nafion component was revealed which is assigned to the motions occurring in the cluster aggregates of side chains [16]. At T > 170 °C an irreversible elongation of the film was observed. The mode peaking in the E' and E'' spectra at about 19 °C was attributed to the mechanical β-relaxation mode. This relaxation is associated with the main-chain motions of the fluorocarbon domains of Nafion [16]. The influence of oxocluster on the mechanical relaxation phenomena of [Nafion/(M_xO_y)$_n$] is more evident in plots of tan δ vs. temperature (Fig. 4). The dynamic mechanical transition temperatures T_α and T_β, respectively, of α- and β-relaxations, were determined accurately fitting tan δ profiles by Gaussian functions (Fig. 4, inset a). It should be observed that T_α: (a) in composite membranes was higher than that of pristine Nafion; (b) increases along the IV group of periodic table ($TiO_2 < ZrO_2 < HfO_2$); and (c) decreases along the VI period ($HfO_2 > Ta_2O_3 > WO_3$). If we consider that the acidity of oxoclusters decreases along the IV group and rises along the VI period, it is expected that depending on the acidity character of M_xO_y nanofillers, the strength of dynamic cross-links, R–SO_3H···M_xO_y···HSO_3–R in polar cages: (a) is stronger in [Nafion/(HfO_2)$_n$]; and (b) decreases as increases the acid character of the filler. The opposite behaviour is observed for T_β (inset b of Fig. 4). Indeed, T_β decreases along the IV group and rises along the VI period.

β-Relaxation of fluorocarbon domains of Nafion corresponds to the solid state transition of pristine polytetrafluoroethylene (PTFE) revealed in the range 19–30 °C. It was reported that at T > 19 °C the PTFE polymer chains mostly exhibits a helical conformation in which 15 CF_2 groups are arranged in seven turns of the helix (15_7) [17,19,20]. Below 19 °C, it was proposed that the helix tightens to a 13_6 conformation in which the chains form an almost regular monoclinic or triclinic structure [17,19,20]. On this basis, it

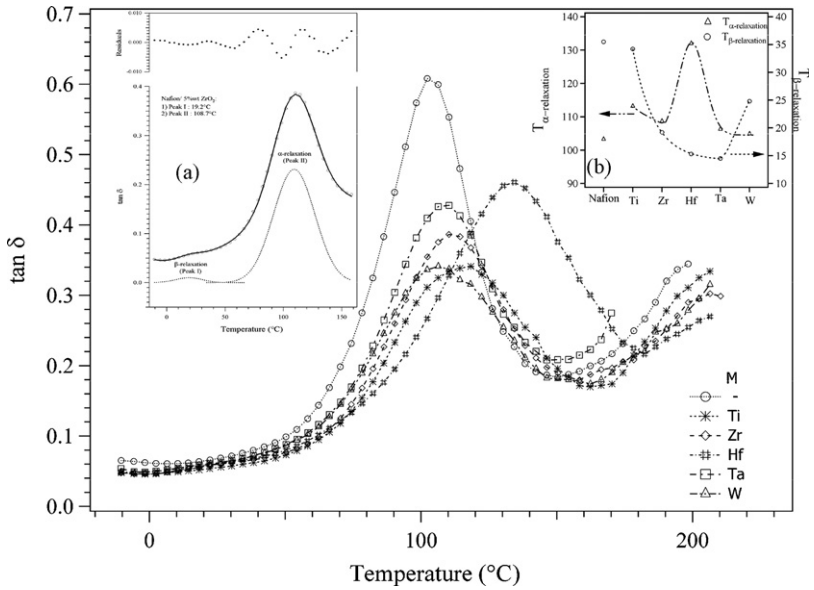

Fig. 4. Tan δ vs. temperature for [Nafion/(M_xO_y)$_n$] with n = 5 wt% and M = Ti, Zr, Hf, Ta and W. The insets report: (a) a typical fitting of α and β relaxation modes; (b) the dependence of T_α and T_β on M. T_α and T_β are the temperatures of peak maxima in spectra of tan δ.

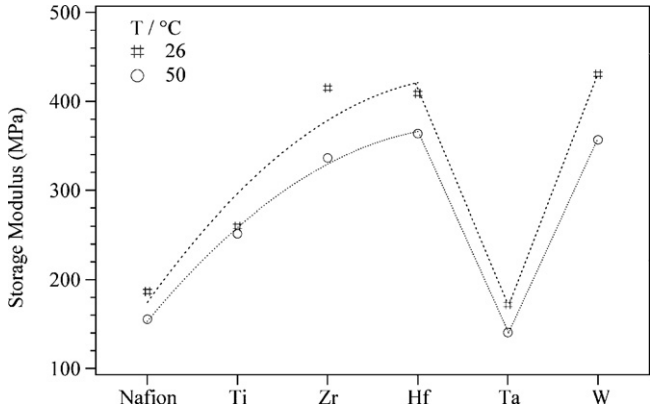

Fig. 5. Dependence on M of the storage modulus measured at 1 Hz and at 50 and 26 °C.

should be proposed that the strength of the interactions occurring in polar cages triggers the fluorocarbon chains present in hydrophobic domains to assume the most stable 15_7 helical conformation thus decreasing T_β along the IV group.

This evidence is in accordance with the dependence on M of the values of storage modulus of [Nafion/$(M_xO_y)_n$] membranes (Fig. 5). As expected, the best mechanical properties are revealed in the [Nafion/$(HfO_2)_n$] material. In particular, the material with the highest strengths in cross-linking interactions ($R–SO_3H\cdots M_xO_y\cdots HSO_3–R$) presents the best mechanical properties owing to the stabilization phenomena of hydrophilic polar clusters and transformation of fluorocarbon chains of hydrophobic domains in the most stable 15_7 helical conformation structure.

Taken together, thermal and DMA results are in accordance with vibrational studies described elsewhere [17] and allowed us to conclude that the concentration and strength of dynamic cross-links occurring inside polar hydrophilic cages of membranes: (a) increase along the IV group and decrease along the VI period; (b) are responsible for the good mechanical and thermal properties of composite membrane based on HfO_2; and (c) modulate the amount of fluorocarbon chains with the 15_7 helical conformation in hydrophobic PTFE domains.

3.3. Broadband dielectric spectroscopy studies

The conductivity and dielectric response of [Nafion/$(M_xO_y)_n$] membranes were investigated by accurate broadband dielectric spectroscopy studies. Fig. 6 shows the dependence on temperature of conductivity (σ_{dc}) of [Nafion/$(M_xO_y)_n$] membranes at 100% RH. σ_{dc} was determined as described elsewhere [15,16] from conductivity Cole–Cole plots. In accordance with studies on the [Nafion/$(SiO_2)_x$] composites [16], profiles of σ_{dc} vs. $1/T$ present three distinct conductivity regions, I, II and III. In I the dependence of σ_{dc} vs. $1/T$ shows the typical Vogel–Tamman–Fulcher behaviour [21–23] thus indicating that segmental motion of the polymer hosts is a crucial factor in the modulation of long-range charge transfer mechanisms. II exhibits Arrhenius-like profiles of σ_{dc} vs. $1/T$. It should be highlighted that cross-linking interactions, $R–SO_3H\cdots M_xO_y\cdots HSO_3–R$, play a crucial role in regulating the conductivity values in region II probably owing to the contribution of the following two concurring effects. The first phenomenon deals with the concentration in bulk materials of charges which are able to migrate and the second event takes into account of host medium relaxation processes. The charges capable of migration are expected to be located in acid water domains. Host dynamics which thermally stimulate the charge migrations are associated with relaxation motions of acid side groups (β-relaxations). As described below, these latter motions are strongly coupled with segmental relaxations of fluorocarbon chains in hydrophobic domains (α-relaxations). In [Nafion/$(HfO_2)_n$], the high concentration of dynamic cross-links: (a) increases the concentration of water acid domains [17]; (b) raises the conductivity owing to the correlation which takes place between β- and α-relaxation events; and (c) improves the thermal stability range of conductivity (SRC) (Table 2). Region III, which describes the temperature range where the materials show a decrease in conductivity as the temperature rises, is observed only for pristine Nafion (Fig. 6). The VTF ($E_{a,VTF}$) and Arrhenius-like ($E_{a,Arrhenius}$) activation energies of [Nafion/$(M_xO_y)_n$] membranes are plotted on M in Fig. 7. $E_{a,Arrhenius}$ is one order of magnitude higher than $E_{a,VTF}$ thus indicating that in region I segmental motion of PTFE plays a crucial role in regulating the proton charge transfer mechanism. In particular, the [Nafion/$(HfO_2)_n$] membrane presents the highest $E_{a,VTF}$ value and the lowest $E_{a,Arrhenius}$. This information, which is in accordance with

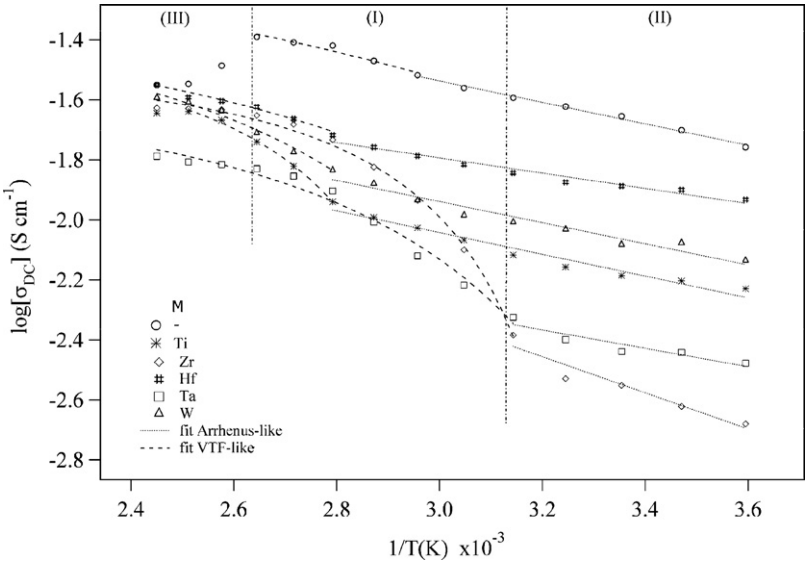

Fig. 6. Dependence of σ_{dc} on $1/T$ for [Nafion/$(M_xO_y)_n$] with n = 5 wt% and M = Ti, Zr, Hf, Ta and W. I, II and III indicate the conductivity regions. VTF and Arrhenius-type fitting curves are shown.

Table 2
Thermal stability range of conductivity (SRC) and conductivity at 135 °C of [Nafion/$(M_xO_y)_n$] membranes with n = 5 wt%.

M_xO_y	SRC[a] (°C)	Conductivity at 135 °C (S cm^{-1})
–	5 < T < 105	2.8×10^{-2}
TiO_2	5 < T < 125	2.3×10^{-2}
ZrO_2	5 < T < 135	2.4×10^{-2}
HfO_2	5 < T < 135	2.8×10^{-2}
Ta_2O_5	5 < T < 135	1.6×10^{-2}
WO_3	5 < T < 135	2.5×10^{-2}

[a] The thermal stability range of conductivity corresponds to the range of temperature in the log(σ) vs. T profiles where at T higher than T = 5 °C is satisfied the following condition: $\partial \log(\sigma)/\partial(1/T) \leq 0$.

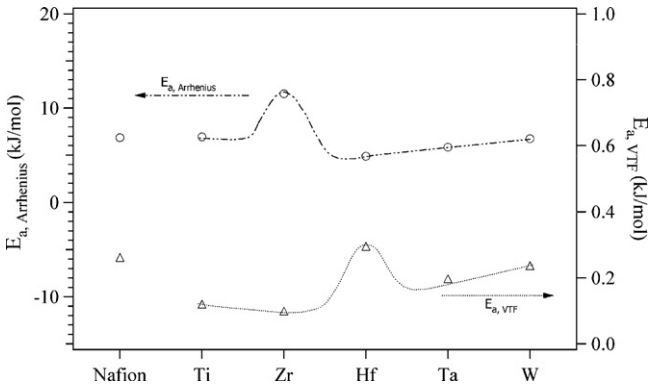

Fig. 7. $E_{a,VTF}$ and $E_{a,Arrhenius}$ vs. M for [Nafion/$(M_xO_y)_n$] with n = 5 wt% and M = Ti, Zr, Hf, Ta and W.

the above-described results, witnesses that the concentration of dynamic cross-links in polar hydrophilic cages of [Nafion/$(HfO_2)_n$] increases the thermal stability of the material and promotes the efficient coupling between α- and β-relaxation modes which are responsible of the improved conductivity of the material.

Table 2 reports the conductivity at 135 °C and the stability range of conductivity of [Nafion/$(M_xO_y)_n$] systems. It should be observed that [Nafion/$(HfO_2)_n$] is the best material in terms of conductivity and SRC parameter. The effect of the host medium relaxation phenomena on the dynamics and charge transfer mechanisms in bulk [Nafion/$(M_xO_y)_n$] membranes was studied by analyzing in detail the complex broadband permittivity spectra of materials. The permittivity spectra ($\varepsilon^*(\omega)$) were obtained by correcting the measured permittivity profiles ($\varepsilon^*_m(\omega)$) by the electrode polarization and σ_{dc} contributions using Eq. (1) [21–25]

$$\varepsilon^*(\omega) = \varepsilon^*_m(\omega) - \frac{\sigma_{dc}(i\omega\tau_{el})^{\gamma}}{i\omega[1+(i\omega\tau_{el})^{\gamma}]} = \varepsilon_\infty + \sum_\infty \frac{\Delta\varepsilon_k}{[1+(i\omega\tau_k)^{\alpha_k}]^{\beta_k}} \quad (1)$$

σ_{dc} is the dc conductivity, α_k and β_k are shape parameters describing the symmetric and asymmetric broadening of the k-th relaxation peak. $\tau_k = (2\pi f_k)^{-1}$ is the dielectric relaxation time (f_k in Hz is the frequency of the peak maximum). $\Delta\varepsilon_k$ is the relaxation strength and τ_{el} is the relaxation time associated with the electrode polarization phenomena.

Selected $\varepsilon^*(\omega)$ permittivity spectra are shown in Fig. 8. In accordance with other studies [16], simulation of $\varepsilon^*(\omega)$ spectra with Eq. (1) revealed two relaxation peaks in the low- and high-frequency wings of the spectra which were attributed respectively to the α- and β-relaxations of Nafion. α-Relaxation is associated with segmental motion of host polymer caused by the diffusion of the

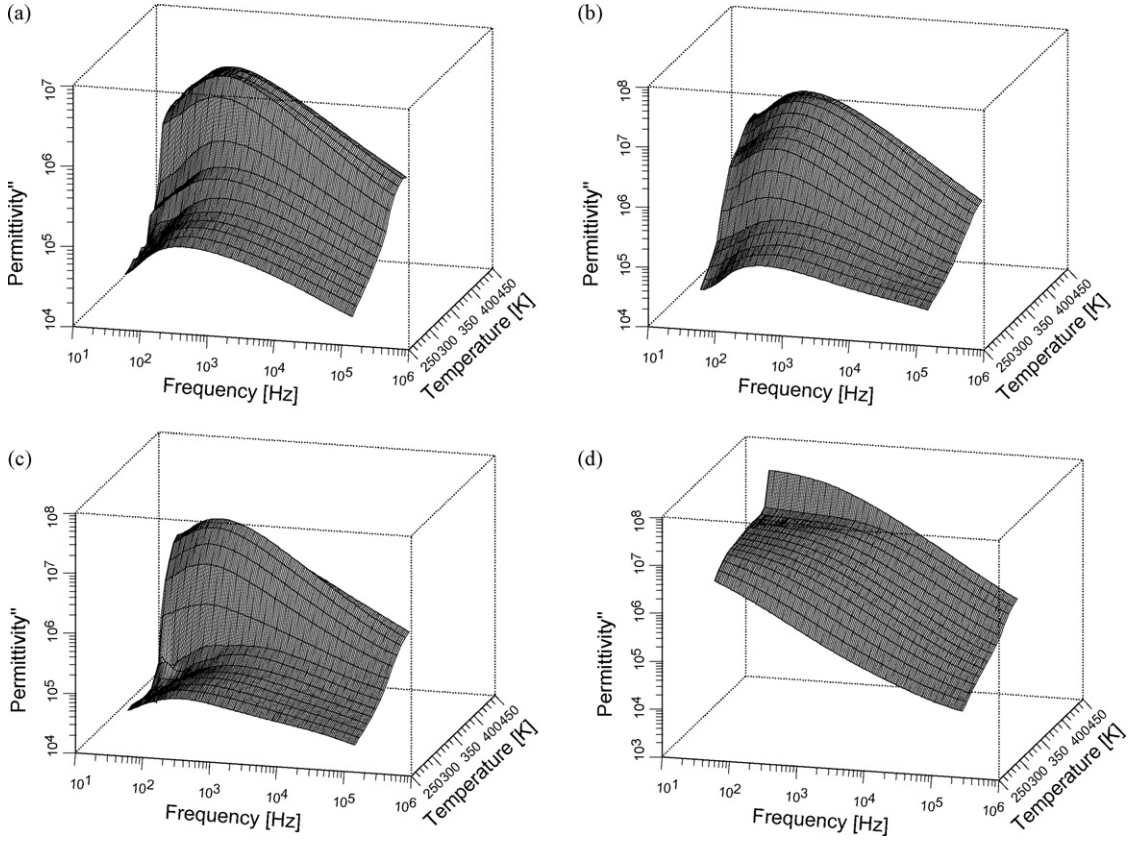

Fig. 8. Imaginary dielectric loss spectra of [Nafion/$(M_xO_y)_n$] with n = 5 wt% and M = Ti, Zr, Hf, Ta and W. Correction of measured permittivity profiles by electrode polarization and σ_{dc} contributions was carried out using Eq. (1).

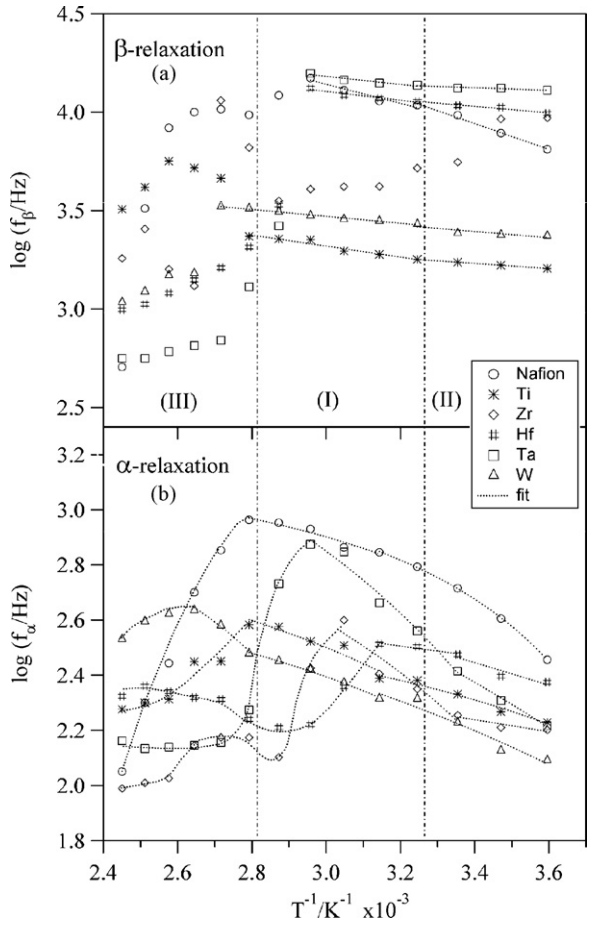

Fig. 9. Dependence of f_α and f_β on $1/T$ in [Nafion/$(M_xO_y)_n$] with n = 5 wt% and M = Ti, Zr, Hf, Ta and W. Regions I, II and III are indicated.

rotational conformational states of fluorocarbon backbone chains in hydrophobic PTFE domains [16]. β-Relaxation is attributed to the local motions resulting from rotational fluctuations of Nafion acid side groups [16].

To reveal the correlations existent between charge migration mechanisms and the polymer bulk relaxations' phenomena, the parameter determined by fitting α and β relaxation peaks with Eq. (1) (Fig. 8) were examined carefully on sample temperature and composition.

Fig. 9 shows the dependence of f_α and f_β on $1/T$. As expected, in regions I and II, f_α presents the well known Vogel–Fulcher–Tamman–Hesse (VFTH) behaviour, while f_β exhibits the typical Arrhenius-like dependence [26,27].

Fig. 10 plots on M the activation energies determined by fitting in regions I and II the frequency curves of α and β relaxation modes showed in Fig. 9. The profiles vs. M of $E_{\alpha,i}$ and $E_{\beta,i}$ resulted very similar to those found in [Nafion/$(SiO_2)_n$] systems [16]. In addition, E_α of materials: (a) increases in the order Ti < Zr < Hf along IV group; and (b) decreases in the order Hf > Ta > W along the VI period. E_β diminishes monotonically in the order: Nafion > Ti > Zr > Hf > Ta > W. This evidence suggests that with respect to pristine Nafion, in composite membranes: (a) segmental motion of fluorocarbon hydrophobic domains, owing to dynamic cross-links occurring in polar ionic cages, is inhibited along the IV group and stimulated along the VI period; (b) the side chain dynamics present values of energy barrier, E_β, which are slightly lower, thus suggesting that in composite membranes flexibility of side groups involved in dynamic cross-links inside hydrophilic polar cages is higher.

The comparison of the $E_{a,Arrhenius}$ and $E_{a,VTF}$ activation energies, shown in Fig. 7, with the values of $E_{\alpha,i}$ and $E_{\beta,i}$, depicted in Fig. 10, reveals the following two characteristics. First, in region I, $E_{a,VTF}$ is one order of magnitude lower than $E_{\alpha,i}$ and $E_{\beta,i}$, thus indicating that the polymer relaxation dynamics are not the rate determining phenomena for the charge transfer migration of [Nafion/$(M_xO_y)_n$] materials. For this reason, in accordance with other studies [16], it should be hypothesized that in I, proton migration occurs owing to a hopping proton exchange mechanism between various water domains present in polar hydrophilic cages interconnected by channels. The shape of water domains is expected to be modulated by the polymer host dynamics. This interpretation explains both the large SRC range and the high conductivity value of [Nafion/$(HfO_2)_n$] material at 135 °C (Table 2).

Second, in region II, $E_{a,Arrhenius}$ is of the same order of magnitude of $E_{\alpha,i}$ and $E_{\beta,i}$ (i = I and II). This information demonstrates that in II the polymer host relaxations are rate determining for proton charge transfer mechanisms. In detail, it should be observed that: (a) $E_{\beta,II}$ decreases in the order Ti > Zr > Hf > Ta > W, thus confirming that, flexibility of side chains in polar ionic cluster of [Nafion/$(M_xO_y)_n$] membranes increases in the same order; (b) $E_{\alpha,II}$ on M, increases along the IV group (Ti < Zr < Hf) and decreases down to the lowest value of $E_{a,Arrhenius}$ along the VI period (Hf > Ta > W). It

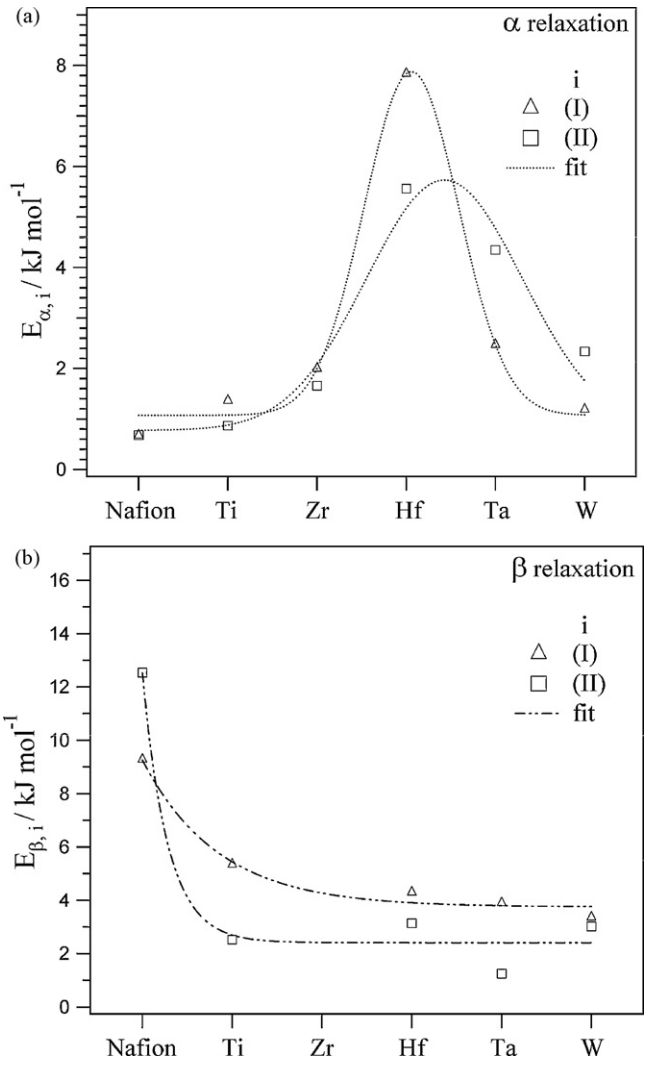

Fig. 10. $E_{\alpha,i}$ and $E_{\beta,i}$ (i = I and II) in regions I and II vs. M for [Nafion/$(M_xO_y)_n$] with n = 5 wt% and M = Ti, Zr, Hf, Ta and W.

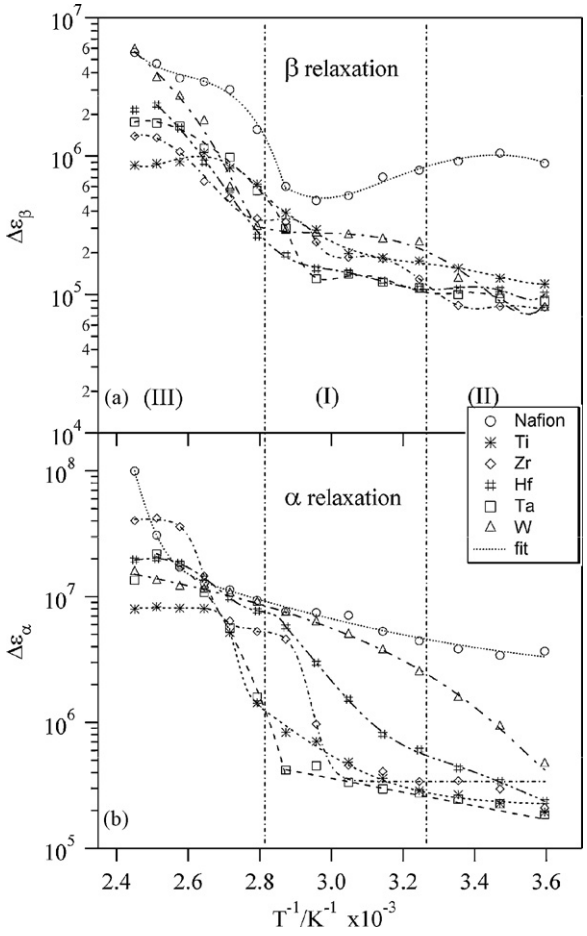

Fig. 11. Dependence on the reciprocal of temperature of the relaxation strengths, $\Delta\varepsilon_\alpha$ and $\Delta\varepsilon_\beta$. Regions I, II and III are indicated.

should be pointed out that [Nafion/$(HfO_2)_n$] membranes: (a) exhibit $E_{\alpha,II} \approx E_{a,Arrhenius}$; and (b) are endowed with $E_{\alpha,II}$ and $E_{a,Arrhenius}$ values corresponding, respectively, to the maximum and the minimum values of the activation energies detected in II for the investigated materials. The results demonstrate that segmental mode relaxations which are coupled with side group relaxations play a crucial role in the modulation of proton charge transfer mechanisms in region II. Indeed, in II the dependence of $E_{\alpha,I}$ on M presents a profile which is in accordance with that of: (a) T_α curve shown in inset b of Fig. 4; (b) the profiles of both the water uptake and ρ, elsewhere reported [17]. ρ is the percentage of PTFE chains with 10_3 helical conformation measured in hydrophobic domains of Nafion [17]. These latter correlations, confirm that in region II the dynamic cross-links between acid side groups and M_xO_y nanofillers are of crucial importance in modulating the thermal, mechanical and electrical properties of the materials.

Fig. 11 plots on temperature the dielectric strengths, $\Delta\varepsilon_\alpha$ and $\Delta\varepsilon_\beta$, of regions I, II and III.

In I and II, $\Delta\varepsilon_\alpha$ and $\Delta\varepsilon_\beta$ values are of about the same order of magnitude and increase monotonically as the temperature rises. This evidence confirms that α and β relaxation modes are strongly coupled with each other. These results, which are in accordance with our previous studies on [Nafion/$(SiO_2)_n$] materials [16], allow us to affirm that [Nafion/$(HfO_2)_n$] presents the best mechanical stability, conductivity and SRC owing to: (a) the high concentration and interaction strength of cross-links in polar ionic cages; and (b) the efficient coupling events between the dynamics of fluorocarbon backbone chains and the highly flexible side groups of Nafion host polymer. In summary, [Nafion/$(HfO_2)_n$] membranes exhibit the best physicochemical properties owing to strong acid–base interactions which take place in polar cages between HfO_2 and sulfonic acid groups of host polymer matrix. Indeed, among the M_xO_y oxoclusters of IV group, HfO_2 is the material with the lowest acidic characteristics [17]. Further insights into the macromolecular dynamics and correlation phenomena between relaxation modes in bulk [Nafion/$(M_xO_y)_n$] materials were obtained by analyzing the

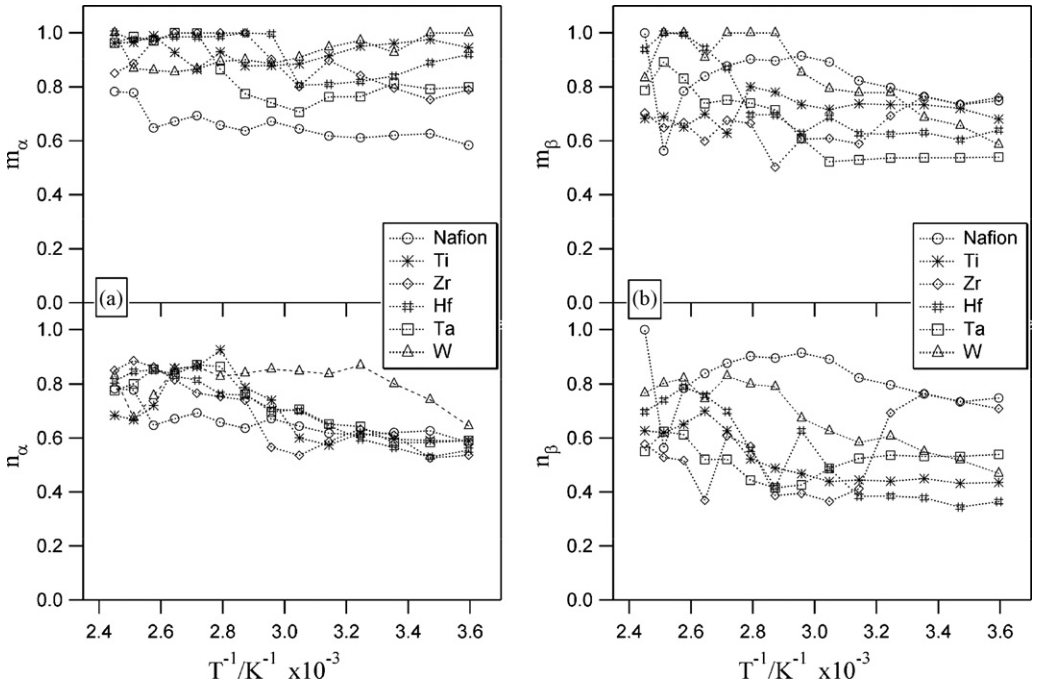

Fig. 12. Dependence on the reciprocal of temperature of the shape parameters *m* and *n* for α- (a) and β-modes (b).

shape parameters m and n of relaxation peaks. $m = \alpha_k$ and $n = \alpha_k\beta_k$. α_k and β_k are fitting parameters obtained as described above by Eq. (1).

Fig. 12 shows that the values of shape parameters n_α and n_β range from 0.6 to 0.8, thus revealing that very strong intermolecular coupling processes occur between the motions of fluorocarbon chains in hydrophobic domains and the dynamics of side chain groups in polar cages of Nafion host polymer [16]. These conclusions, which are further supported by the values lower than 1 of m_α and m_β parameters, demonstrate clearly that the cross-linking phenomena occurring inside ionic polar cluster influence significantly the local motion of acid side groups and the segmental relaxation events of hydrophobic PTFE domains of materials.

In summary, M_xO_y nanofillers play an important role in stabilizing both the hydrophobic and the hydrophilic domains of materials and in tuning the proton charge transfer processes in polar hydrophilic cages and in their interconnecting channels. In accordance with literature [16], the charge transfer mechanism in the investigated materials is modulated by two overall relaxation phenomena strongly coupled with each other which are indicated as R_c and R_{fd}. R_c is the cage relaxation event, which accounts of the correlated molecular dynamics occurring inside hydrophilic domain of materials. R_{fd} is the general relaxation mode accounting of the motions of fluorocarbon chains in hydrophobic domains of Nafion host polymer.

BDS results allow us to admit that conductivity in [Nafion/$(M_xO_y)_n$] systems occurs owing to proton hopping processes inside polar clusters and interconnecting channels which are mediated by: (a) the concentration of interstitial free water; (b) the concentration of acid side groups; (c) the concentration and strength of R–SO_3H···M_xO_y···HSO_3–R cross-links; and (d) segmental motion of fluorocarbon backbone domains. The results are in accordance with studies on [Nafion/$(SiO_2)_x$] materials [16] and confirm that the conductivity in [Nafion/$(M_xO_y)_n$] membranes takes place owing to the previously proposed *peristaltic*-like mechanism [16]. In this latter mechanism, long range charge migrations by hopping processes happen when different water domains intersect with each other owing to fluctuations in polar cages of side groups strongly coupled with the relaxation motions of PTFE chains in hydrophobic domains of Nafion host polymers.

4. Conclusions

Described in this paper are the results of studies on five [Nafion/$(M_xO_y)_n$] (M = Ti, Zr, Hf, Ta and W) membranes. These studies were performed with the aim of elucidating the conductivity mechanism and the relaxation processes characterizing the properties of composite materials.

MDSC profiles showed that I, II and III thermal transitions were detected in the temperature range 90–300 °C. I is associated with an order–disorder transition of polar ionic clusters of Nafion. II is ascribed to the decomposition of –SO_3H acid groups. III corresponds to the order–disorder transition occurring in microcrystalline regions of hydrophobic PTFE domains of Nafion.

DMA analyses showed that materials are characterized by α and β mechanical relaxation events. α-Mechanical mode is measured at 100 °C and is attributed to the relaxation of cluster aggregates of Nafion side chains. β-Relaxation, revealed at about 19 °C, corresponds to the main chain motion in PTFE domains of Nafion.

The electric properties and conductivity mechanism of membranes were studied by broadband dielectric spectroscopy in the frequency and temperature range respectively of 40 Hz–10 MHz and 5–135 °C. α and β dielectric relaxation phenomena were revealed in [Nafion/$(M_xO_y)_n$] membranes. α mode was measured at low frequencies and attributed to segmental motion of fluorocarbon chains in PTFE hydrophobic domains of Nafion. β-Relaxation was revealed at high frequencies and was associated with the dynamics of acid side chains of Nafion. α and β relaxations are strongly coupled to each other and are diagnostic for the effect of the various M_xO_y oxoclusters on the properties of [Nafion/$(M_xO_y)_n$] membranes. In particular, M_xO_y influences the properties of membranes owing to the formation of dynamic cross-links R–SO_3H···M_xO_y···HSO_3–R which modulate the mechanical, thermal and dynamical characteristics of Nafion host polymer. Finally, the SRC parameter of $5\,^\circ C \le T \le 135\,^\circ C$ and the conductivity value of 2.8×10^{-2} S cm^{-1} at 135 °C and 100% RH classifies [Nafion/$(HfO_2)_n$] as a very promising proton conducting membrane to use in DMFCs and PEMFCs.

In conclusion, the combined studies carried out simultaneously by DMA, MDSC, and BDS measurements allowed us to propose that in [Nafion/$(M_xO_y)_n$] membranes proton migration along interconnecting channels and polar hydrophilic clusters occurs owing to a *peristaltic*-like mechanism. In this conductivity mechanism protons are exchanged between different fluctuating water species domains through hopping processes. The shape changes and water domain fluctuations are modulated by the α and β relaxations of Nafion host polymer.

Acknowledgements

Research was funded by the Italian MURST project NUME of FISR2003, “Sviluppo di membrane protoniche composite e di configurazioni elettrodiche innovative per celle a combustibile con elettrolita polimerico”.

References

[1] J. Larminie, A. Dicks, Fuel Cell Systems Explained, J. Wiley and Sons, Chichester, 2000.
[2] J.M. Ogden, in: W. Vielstich, A. Lamm, H.A. Gasteiger (Eds.), Handbook of Fuel Cells: Fundamentals, Technology and Applications, vol. 3, Wiley, Chichester, 2003, p. 3.
[3] T. Theisen, in: W. Vielstich, A. Lamm, H.A. Gasteiger (Eds.), Handbook of Fuel Cells: Fundamentals, Technology and Applications, vol. 3, Wiley, Chichester, 2003, p. 25.
[4] A.J. Appleby, Sci. Am. 28 (1999) 74.
[5] S.J.C. Cleghorn, X. Ren, T.E. Springer, M.S. Wilson, C. Zawodzinski, T.A. Zawodzinski, S. Gottesfeld, Int. J. Hydrogen Energy 22 (1997) 1137.
[6] K.D. Kreuer, J. Membr. Sci. 185 (2001) 29.
[7] G. Alberti, M. Casciola, Solid State Ionics 145 (2001) 3.
[8] K.A. Mauritz, R.B. Moore, Chem. Rev. 104 (2004) 4535.
[9] M. Neergat, K.A. Friedrich, U. Stimming, in: W. Vielstich, A. Lamm, H.A. Gasteiger (Eds.), Handbook of Fuel Cells: Fundamentals, Technology and Applications, vol. 4, Wiley, Chichester, 2003, p. 856.
[10] M. Nakao, M. Yoshitake, in: W. Vielstich, A. Lamm, H.A. Gasteiger (Eds.), Handbook of Fuel Cells: Fundamentals, Technology and Applications, vol. 3, Wiley, Chichester, 2003, p. 412.
[11] G. Alberti, M. Casciola, Annu. Rev. Mater. Res. 33 (2003) 129.
[12] K.A. Mauritz, Mater. Sci. Eng. C 6 (1998) 121.
[13] I. Honma, H. Nakajima, O. Nishikawa, T. Sugimoto, S. Nomura, Solid State Ionics 162 (2003) 237.
[14] V. Di Noto, M. Vittadello, Electrochim. Acta 50 (2005) 3998.
[15] V. Di Noto, M. Vittadello, R.P.J. Jayakody, A.N. Khalfan, S.G. Greenbaum, Electrochim. Acta 50 (2005) 4007.
[16] V. Di Noto, R. Gliubizzi, E. Negro, G. Pace, J. Phys. Chem. B 110 (2006) 24972.
[17] V. Di Noto, R. Gliubizzi, E. Negro, M. Vittadello, G. Pace, Electrochim. Acta 53 (2007) 1618.
[18] V. Di Noto, M. Vittadello, V. Zago, G. Pace, M. Vidali, Electrochim. Acta 51 (2006) 1602.
[19] G. Zerbi, M. Sacchi, Macromolecules 6 (1973) 692.
[20] G. Masetti, F. Cabassi, G. Morelli, G. Zerbi, Macromolecules 6 (1973) 700.
[21] M. Vittadello, S. Suarez, K. Fujimoto, V. Di Noto, S.G. Greenbaum, T. Furukawa, J. Electrochem. Soc. 152 (2005) A956.
[22] V. Di Noto, J. Phys. Chem. B 106 (2002) 11139.

[23] V. Di Noto, M. Vittadello, S.G. Greenbaum, S. Suarez, K. Kano, T. Furukawa, J. Phys. Chem. B 108 (2004) 18832.
[24] T. Furukawa, M. Imura, H. Yuruzume, Jpn. J. Appl. Phys. 36 (1997) 1119.
[25] K. Kano, Y. Takahashi, T. Furukawa, Jpn. J. Appl. Phys. 40 (2001) 3246.
[26] A. Schönhals, in: J.P. Runt, J.J. Fitzgerald (Eds.), Dielectric Spectroscopy of Polymeric Materials, American Chemical Society, Washington, DC, 1997, p. 81.
[27] A. Schönhals, in: F. Kremer, A. Schönhals (Eds.), Broadband Dielectric Spectroscopy, Springer-Verlag, Berlin, Germany, 2003, p. 225.